Acta Crystallographica Section D
Biological Crystallography
ISSN 0907-4449

Crystallization and preliminary X-ray crystallographic studies on a Fab fragment of the mouse anti-human Fas monoclonal antibody HFE7A

Shuichiro Ito,* Tomoko Takayama, Hiroyuki Hanzawa, Kimihisa Ichikawa, Jun Ohsumi, Nobufusa Serizawa, Hideyuki Haruyama and Tadashi Hata

Biomedical Research Laboratories, Sankyo Co. Ltd, 1-2-58 Hiromachi, Shinagawa-ku, Tokyo 140-8710, Japan

Correspondence e-mail: shuici@shina.sankyo.co.jp

Received 17 April 2001
Accepted 6 August 2001

The Fas–Fas ligand system is involved in apoptosis. The mouse anti-human Fas monoclonal antibody HFE7A (m-HFE7A) has a potential use in human therapy against autoimmune diseases such as rheumatoid arthritis. Information on the three-dimensional structure is essential for antibody humanization. Crystals of an antigen-binding fragment (Fab) of m-HFE7A were obtained by the hanging-drop vapour-diffusion method using sodium citrate as a precipitant and 2-methyl-2,4-pentanediol as an additive. Fast optimization to produce single crystals suitable for X-ray analysis was achieved by the streak-seeding technique. The crystals belong to the orthorhombic space group $P2_12_12_1$, with unit-cell parameters $a = 43.4$, $b = 74.0$, $c = 133.8$ Å. The crystals diffract at least to 2.5 Å resolution.

1. Introduction

Apoptosis, or programmed cell death, is involved in many biological processes such as development of the immune system and maintenance of tissue homeostasis (Nagata, 1997). Binding of Fas ligand (FasL) or agonistic antibodies to Fas induces apoptosis (Yonehara *et al.*, 1989; Itoh *et al.*, 1991; Suda *et al.*, 1993). Mice with mutations of Fas and/or FasL develop massive lymphadenopathy and autoimmune diseases, which indicates that the Fas–FasL system plays an important role in the elimination of autoreactive lymphoid cells (Watanabe-Fukunaga *et al.*, 1992; Takahashi *et al.*, 1994).

The mouse antibody HFE7A (m-HFE7A), raised against human Fas, binds to both human and mouse Fas (Ichikawa *et al.*, 2000; Yoshida-Kato *et al.*, 2000). Administration of m-HFE7A induces apoptosis in thymocytes in mice. However, m-HFE7A shows no sign of hepatotoxicity in mice, which is observed in the case of the hamster anti-mouse Fas monoclonal antibody Jo-2 (Ogasawara *et al.*, 1993). Moreover, the administration of m-HFE7A to mice blocks the injury to the liver induced by Jo-2. Therefore, m-HFE7A may provide a useful therapy for the treatment of autoimmune diseases such as rheumatoid arthritis and fulminant hepatitis.

Humanization is a procedure required to enable murine antibodies to be used in human therapy, since murine antibodies are immunogenic in human (Queen *et al.*, 1989). It is important to graft both residues in the complementarity-determining region (CDR), which is mainly involved in antigen binding, and a small number of residues maintaining the conformation of the CDR residues. Information on the three-dimensional structure is essential to limit the number of murine residues to as few as possible and reduce immunogenicity. The antibody m-HFE7A has been humanized using a model built by homology modelling described elsewhere and a humanized HFE7A antibody is currently under development for human therapy.

To further understand antibody humanization and ultimately elucidate the mechanism of apoptosis induced by agonistic antibodies, crystallization of the m-HFE7A Fab was performed. We also report an application of the streak-seeding technique (Stura & Wilson, 1991) to accelerate the speed and optimize the crystallization conditions.

2. Material and methods

2.1. Preparation of the Fab

Production and purification of m-HFE7A (IgG1, κ light chain) were carried out as described previously (Ichikawa *et al.*, 2000). The Fab fragment of m-HFE7A was prepared by papain cleavage followed by limited reduction with dithiothreitol (DTT) through the $F(ab)_2$ fragment of IgG. The IgG purified with a Protein-G column was dialyzed against phosphate-buffered saline containing 75 m*M* phosphate pH 7.2 and 75 m*M* NaCl. The IgG (10 mg ml^{-1}) was then cleaved to $F(ab)_2$ by papain using a 1:100(*w*/*w*) ratio of papain to IgG in the presence of 0.1 m*M* L-cysteine at 310 K for 4 h. The reaction was stopped by the addition of *N*-ethylmaleimide to a final concentration of 30 m*M*. The $F(ab)_2$ fragment was isolated by gel filtration using a Superdex

200 column (Pharmacia) with phosphate-buffered saline containing 150 m*M* phosphate pH 7.2 and 10 m*M* NaCl. The pooled fraction was raised to pH 8.0 with NaOH and reduced at 310 K for 30 min with DTT to a final concentration of 10 m*M*. The reduction was stopped by adding iodoacetamide to 10 m*M*. The Fab was dialyzed against 10 m*M* Tris–HCl pH 7.4 and concentrated to 10 mg ml^{-1}. The protein was tested for purity at each step by SDS–PAGE under reduced and non-reduced conditions and by gel filtration. The distribution of apparent molecular weight for the Fab was measured by dynamic light scattering on a DynaPro-801 instrument (Protein Solutions).

2.2. Crystallization and preliminary X-ray diffraction analysis

The initial screening for crystallization of the Fab was carried out by the hanging-drop vapour-diffusion method at 277, 286 and 296 K. 2 µl of the protein solution was mixed with 2 µl of a precipitant solution containing 1.2 *M* sodium citrate, 3% 2-methyl-2,4-pentanediol (MPD) and 10 m*M* sodium borate pH 8.5. Incubation at 296 K for five weeks produced stacked crystals. Crystals suitable for X-ray analysis were obtained by the streak-seeding technique from a drop incubated for 6 h after mixing 3 µl of the protein solution with 5 µl of a precipitant solution containing 1.2 *M* sodium citrate in 10 m*M* sodium borate pH 8.5 at 296 K. The crystals appeared in a few days and reached maximum dimensions of 0.35 × 0.25 × 0.2 mm in one week (Fig. 1).

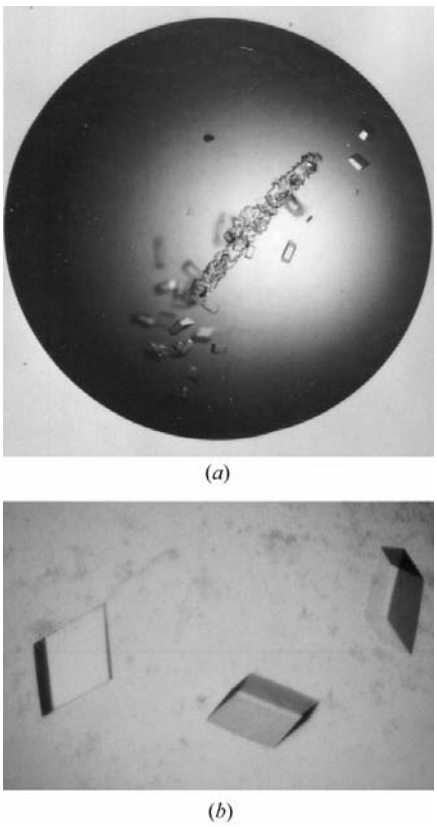

Figure 1
(*a*) The microcrystals after the initial streak seeding. (*b*) The crystals after the optimization for the pre-equilibrium conditions and the seed stock solution. The dimensions of the crystals are approximately 0.35 × 0.25 × 0.2 mm.

Diffraction data were measured at room temperature from a single crystal placed in a thin-walled glass capillary tube. Preliminary intensity data were collected on an R-AXIS IV imaging-plate detector system using Cu $K\alpha$ radiation produced by a Rigaku rotating-anode generator and were processed with *DENZO* and *SCALEPACK* (Otwinowski & Minor, 1997).

3. Results and discussion

3.1. Crystallization

The initial screenings to determine the crystallization conditions included the sparse-matrix method (Jancarik & Kim, 1991), the low ionic strength screen (Harris *et al.*, 1995) and the footprint screen (Stura *et al.*, 1992). Although the light-scattering data showed that the Fab was narrow unimodal (data not shown), indicating a relatively high possibility for the protein to crystallize (D'Arcy, 1994), even small crystals were not obtained in these initial screenings. MPD was then used as an additive and its effect on nucleation was evaluated. A particle appeared together with precipitate in a drop equilibrated against precipitant solution containing 1.2 *M* sodium citrate, 10 m*M* sodium borate pH 8.5 and 3% MPD five weeks after setting the drop. The particle showed birefringence. However, it was difficult to recognize whether or not it was crystalline using a microscope. The streak-seeding technique was applied to analyze it further. Using a probe consisting of a cat whisker, the particle was transferred into a drop equilibrated against precipitant solution containing 1.0 *M* sodium citrate and 10 m*M* sodium borate pH 8.5, which had remained clear for seven weeks after setting the drop. Small crystals appeared within 1 d with good morphology (Fig. 1). The small crystals were then crushed and a solution containing the crushed crystals was used in the subsequent streak seeding to determine the pre-equilibrium conditions of the protein-precipitant solution prior to seeding. As mentioned in the crystallization experiments, MPD was essential for spontaneous nucleation. The pre-equilibrium conditions were refined using a precipitant solution without MPD to avoid spontaneous nucleation. In the refinement, drops consisting of 3 µl of protein solution mixed with 5 µl of precipitant solution were used to shorten the incubation time. After optimizing the pre-equilibrium conditions, a final seed solution was prepared to produce crystals suitable for X-ray analysis by a serial dilution of the initial seed solution. Using the streak-seeding technique, it took only two weeks from the first appearance of the particles to the collection of the preliminary diffraction data described below.

3.2. Preliminary X-ray diffraction analysis

The crystals belong to the orthorhombic space group $P2_12_12_1$, with unit-cell parameters a = 43.4, b = 74.0, c = 133.8 Å. Assuming the presence of one molecule in the asymmetric unit, the calculated value of crystal volume per protein mass (V_M) (Matthews, 1968) is 2.2 Å^3 Da^{-1}. A total of 62 479 observations were measured and 9072 independent reflections were obtained with an $R_{merge}(I)$ of 0.063 and a completeness of 99.5% to a resolution of 3.0 Å. Although the crystals diffracted at least to 2.5 Å resolution, severe radiation damage was observed. Further efforts such as data collection at low temperature and/or at high speed with synchrotron radiation will be necessary to collect data at higher resolution.

Using the streak-seeding technique, we were able to obtain and optimize the crystallization conditions suitable for X-ray analysis in a short period. Although high-throughput screening with an automated robot can test many types of precipitants for a large number of proteins at a high speed, a crystallization robot cannot perform procedures which require such skill. Therefore, the seeding technique is valuable for certain proteins when standard screening fails.

SI and TH are members of the Structural Biology Sakabe Project (SBSP) of the Foundation for Advanced of International Science (FAIS).

References

D'Arcy, A. (1994). *Acta Cryst.* D**50**, 469–471.
Harris, L. J., Skaletsky, E. & McPherson, A. (1995). *Proteins*, **23**, 285–289.
Ichikawa, K., Yoshida-Kato, H., Ohtsuki, M., Ohsumi, J., Yamaguchi, J., Takahashi, S., Tani, Y., Watanabe, M., Shiraishi, A., Nishioka, K., Yonehara, S. & Serizawa, N. (2000). *Int. Immunol.* **12**, 555–562.
Itoh, N., Yonehara, S., Ishii, A., Yonehara, M.,

Mizushima, S., Sameshima, M., Hase, A., Seto, Y. & Nagata, S. (1991). *Cell*, **66**, 233–243.
Jancarik, J. & Kim, S.-H. (1991). *J. Appl. Cryst.* **24**, 409–411.
Matthews, B. W. (1968). *J. Mol. Biol.* **33**, 491–497.
Nagata, S. (1997). *Cell*, **88**, 355–365.
Ogasawara, J., Watanabe-Fukunaga. R., Adachi, M., Matsuzawa, A., Kasugai, T., Kitamura, Y., Itoh, N., Suda, T. & Nagata, S. (1993). *Nature (London)*, **364**, 806–809.
Otwinowski, Z. & Minor, W. (1997). *Methods Enzymol.* **276**, 307–326.
Queen, C., Schneider, W. P., Selick, H. E., Payne, P. W., Landolfi, N. F., Duncan, J. F., Avdalovic, N. M., Levitt, M., Junghans, R. P. & Waldmann, T. A. (1989). *Proc. Natl Acad. Sci. USA*, **86**, 10029–10033.
Stura, E. A. & Wilson, I. A. (1991). *J. Cryst. Growth*, **110**, 270–282.
Stura, E. A., Nemerow, G. R. & Wilson, I. A. (1992). *J. Cryst. Growth*, **122**, 273–285.
Suda, T., Takahashi, T., Golstein, P. & Nagata, S. (1993). *Cell*, **75**, 1169–1178.
Takahashi, T., Tanaka, M., Brannan, C. I., Jenkins, N. A., Copeland, N. G., Suda, T. & Nagata, S. (1994). *Cell*, **76**, 969–976.
Watanabe-Fukunaga, R., Brannan, C. I., Copeland, N. G., Jenkins, N. A. & Nagata, S. (1992). *Nature (London)*, **356**, 314–317.
Yonehara, S., Ishii, A. & Yonehara, M. (1989). *J. Exp. Med.* **169**, 1747–1756.
Yoshida-Kato, H., Ichikawa, K., Yamaguchi, J., Watanabe, K., Ohsumi, J., Yonehara, S. & Serizawa, N. (2000). *Biosci. Biotechnol. Biochem.* **64**, 1903–1908.